EUMETSAT STUDY FOR ATTITUDE DYNAMICS AND DISTURBANCES IN LEO AND GEO ENVIRONMENT

Pessina S. [(1)], **Gomes Paulino N.M.G.** [(2)], **De Juana J.M.** [(1)], **Righetti P.** [(1)]

[(1)] *EUMETSAT, Eumetsat Allee 1, Darmstadt, D-64295 Germany +49 6151-807-7*

Stefano.Pessina@eumetsat.int, Jose.DeJuana@eumetsat.int, Pierluigi.Righetti@eumetsat.int

[(2)] *GMV, Isaac Newton 11 P.T.M., Tres Cantos, 28760 Madrid, Spain; Tel. +34 918072100*

npaulino@gmv.com

Abstract: *To support both mission analyses of the future programmes and the in-flight analyses for the currently flying satellites, EUMETSAT implemented a dedicated study with the following objectives:*

- *To model the dynamic loads induced by the space environment (according to ECSS Space Environment standards) for gravity gradient, radiation pressure, air drag and magnetic field, based on prescribed orbits and attitude laws, characteristic of current and future EUMETSAT satellites, both for LEO and GEO*
- *Assuming multiple reaction wheels control for the spacecraft, to characterise the wheel off-loading frequency/needs, based on angular momentum accumulation*
- *To predict and analyse the blinding/occultation by Sun/Moon/Earth of instruments (such as star-trackers), together with solar-array(s) illumination.*

A first study case is for LEO environment based on the currently flying EPS satellite: it analyses various solar activity profiles and orbit altitude: this allowed both to characterise the seasonal and long term trends in the satellite observed dynamics, but also to have an internal evaluation of the torque load in view of the foreseen satellite end-of-life deorbiting.

A second study case is for GEO environment based on the future MTG satellite: it analyses various orbital inclinations, mission phases and year of operations, including regular 180 deg yaw-flip manoeuvres: this allowed characterising the variable need of thrusters' based off-loading of the reaction wheels during the mission and the subsequent impact on the orbit control for station keeping, due to thrusters misalignment and aging dependant plume impingement.

Keywords: *Attitude Dynamics, Environment Torques, Wheels off-loading, Star-trackers blinding*

1. Acronym list

AADD= Analysis of Attitude Disturbances and Dynamics

LEO=Low Earth Orbit	EPS=EUMETSAT Polar System
GEO=Geosynchronous	FD=Flight Dynamics
GBF=Geometric Body Frame	CoM=Centre of Mass
SC=Spacecraft	SA=Solar Array
CB=Central Body	SCF=Spacecraft Frame
ECI=Earth Centre Inertial frame (J2000)	ECEF=Earth Centred Earth fixed frame
MSFC=Marshall Space Flight Center	RCS=Reaction Control System

2. Introduction

EUMETSAT is the "EUropean organisation for the exploitation of METeorological SATellites". It is an independent intergovernmental organisation created in 1986 to establish, maintain and exploit European systems of operational meteorological satellites. It currently operates a system of meteorological satellites, monitoring the atmosphere and ocean and land surfaces which deliver weather and climate-related satellite data, images and products – 24 hours a day, 365 days a year (see [1]). EUMETSAT currently has seven operational weather satellites. Meteosat-7,-8, 9 and 10, Metop-A, -B and Jason-2. Meteosat are the satellites of the geosynchronous (GEO) fleet. There are two generations of active Meteosat satellites, Meteosat First Generation (MFG) and Meteosat Second Generation (MSG). Metop are low-Earth orbit (LEO) polar meteorological satellites, which form the space segment component of the overall EUMETSAT Polar System (EPS). Jason-2 reliably delivers detailed oceanographic data vital to our understanding of weather forecasting and climate change monitoring. The currently flying EUMETSAT satellites, missions and their orbits is briefly shown in Figure 1.

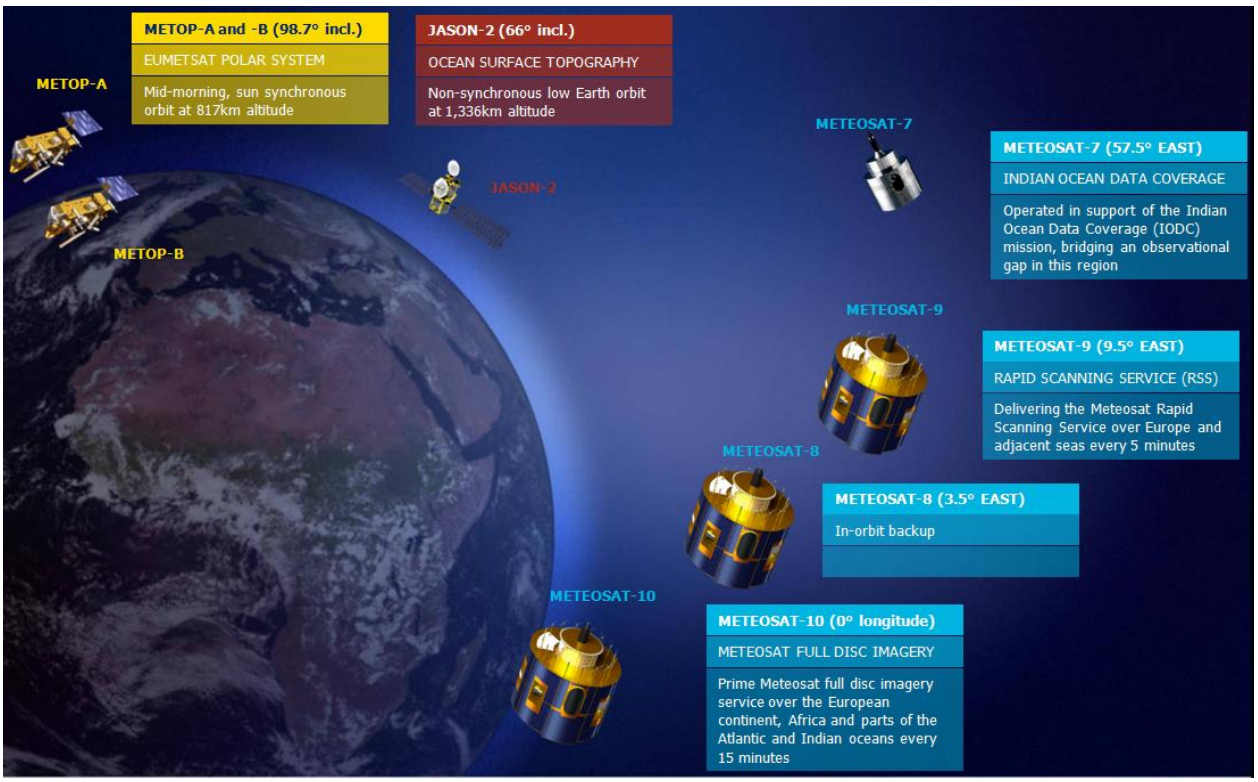

Figure 1. EUMETSAT currently flying satellites

3. Study objectives

The Analysis of Attitude Disturbances and Dynamics Tool (AADD-Tool) is prototyped and used in the EUMETSAT-AADD project to analyse the disturbances impacts on attitude of the spacecraft, start tracker blinding, momentum unloading schemes, and solar power supply.
The following is the list of objectives of the study:

1. First objective of this study is the modelling of dynamic loads induced by the space environment (according to ECSS Space Environment standards) for gravity gradient, radiation pressure, air drag and magnetic field. The models shall be based on prescribed orbits and attitude laws, characteristic of current and future EUMETSAT satellites. The models shall consider a limited set of satellite surfaces, shape and mass distribution, together with sensors and actuators, as necessary for allowing the performance analyses requested by this study.
2. Assuming a spacecraft controlled with reaction wheels, second objective of the study is the characterisation wheel off-loading frequency/needs, based on angular momentum accumulation in the spacecraft body frame. This is based on:
    a. Analysis of the wheel de-saturation schemes considering both regular wheel off-loadings at fixed intervals or maximisation of intervals between off-loadings; of special interest shall be the residual delta-V's induced by wheel off-loading manoeuvres.
    b. Analysis of the external disturbance torques characterisation, including impacts on wheel de-saturation and actuator capacity for different orbit altitudes, eccentricities and solar activities.
3. Third objective of this study is the prediction and analyses of star-trackers blinding/occultation, together with solar-array(s) illumination. This is based on:
    a. Characterisation of star-trackers boresight to Sun/Moon/Earth(limb) angles, with prediction of eventual blinding/occultation events of instruments (i.e. star tracker).
    b. Characterisation of Sun incidence on solar arrays.
4. For achieving the study objectives, a specific tool shall be prototyped and validated, using as much as possible independent simulation models or directly flight data.

4. Tool architecture

The tool is developed in Matlab/Simulink environment, and its architecture is based on four processes:

- Main GUI – principal interface of the user to setup the case study (spacecraft geometry, simulation, selection of attitude and disturbances)
- Config – This process parses the user input to create the spacecraft mesh, initialize the simulator data and set the input and output files. The project data saved in a global variable AADDTool accessible to all the processes in the tool.
- Mission – This process runs the analysis accordingly to the configuration set by the user. A template in Simulink is initialized and run, using the configuration in AADDTool . The main outputs of this process are the .mat files with the outputs from the analysis.
- Display – This process is launched to post process the analysis data, generate the signal statistics, organize the data and display the figures. A folder is also created to store the project data and store the simulation and output data files.

The interaction of these processes is summarized in Figure 2.

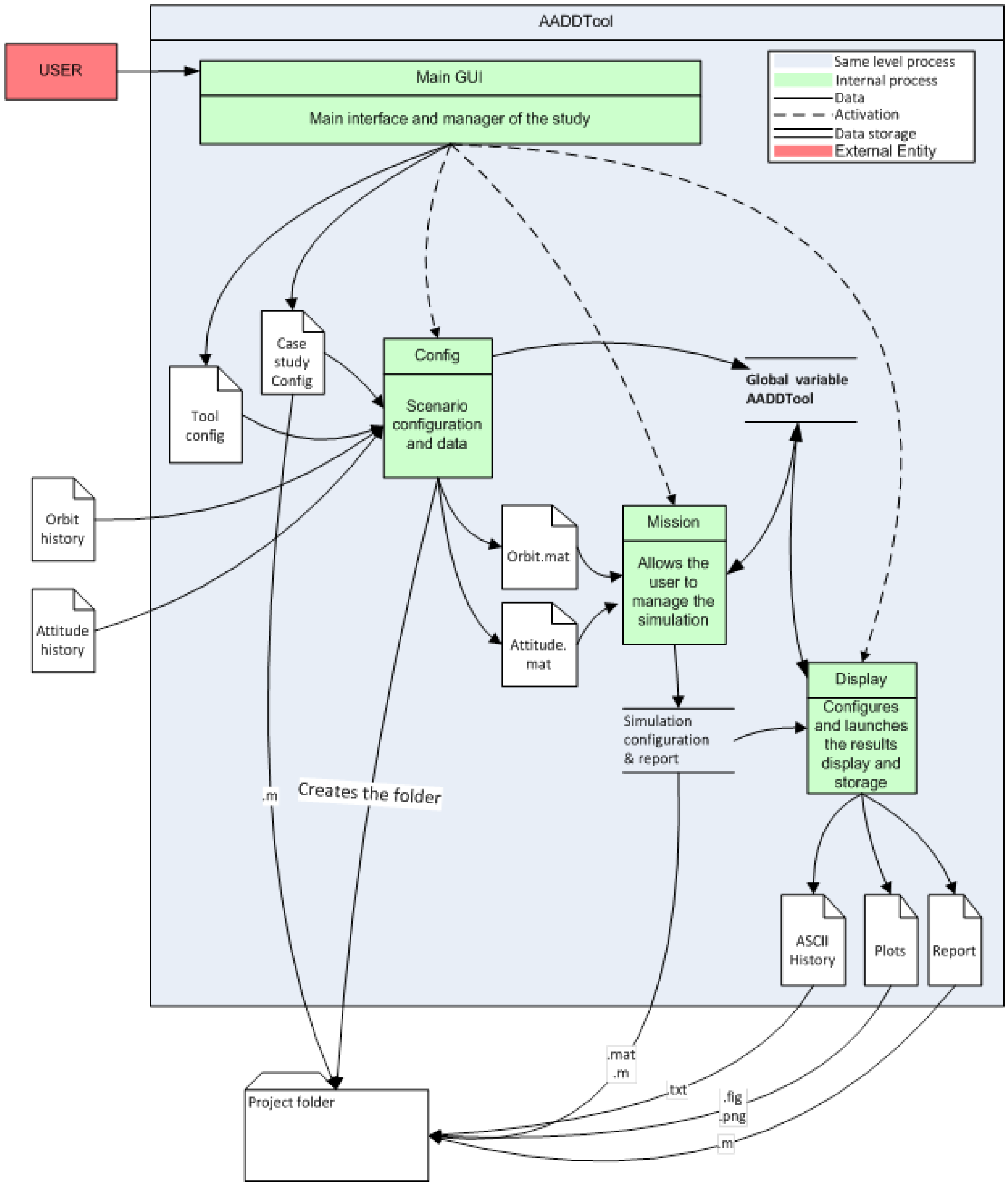

Figure 2. AADD tool architecture

5. Detailed design

The details of the models implemented in the AADD-tool are here briefly mentioned. Full details, including algorithmic implementation, can be found in the software design document (see [2])

5.1. Geometry configuration

An important task is the construction of the spacecraft geometry and mesh. This is described in more detail in the following sub-section. The user's selections, summary of the simulation and preview of the spacecraft geometry is shown in the GUI, to be visible to the user before starting the mission simulation.

The spacecraft model is constituted by the central body and 1 or 2 rectangular solar panels. The central body is configured as a prism where the top and bottom areas can be different, see Figure 3 (left). These are defined in the geometric frame of the spacecraft (GBF). The solar panels are modelled as rectangular surfaces attached to the main body at a pivot point, see Figure 3 (right).

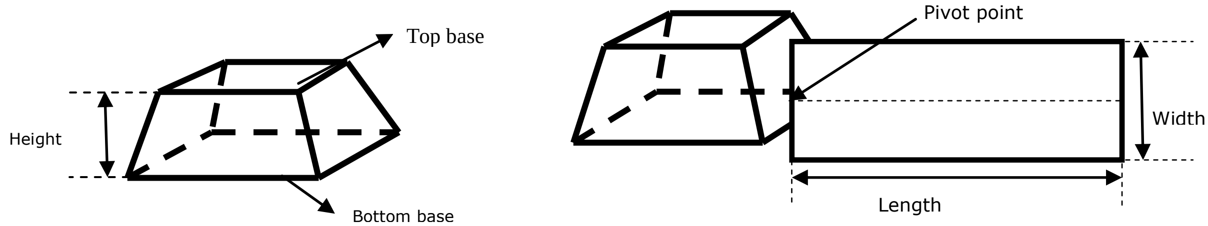

Figure 3. Central body geometry (left) and Geometry of the solar panel (right)

Recovering the definitions of the tilt and rotation angles of the solar panels, Figure 4, an auxiliary intermediary frame is defined between the geometric frame of the central body and the solar panel element. These rotations are defined in the solar panel reference frame (SPF) previously defined.

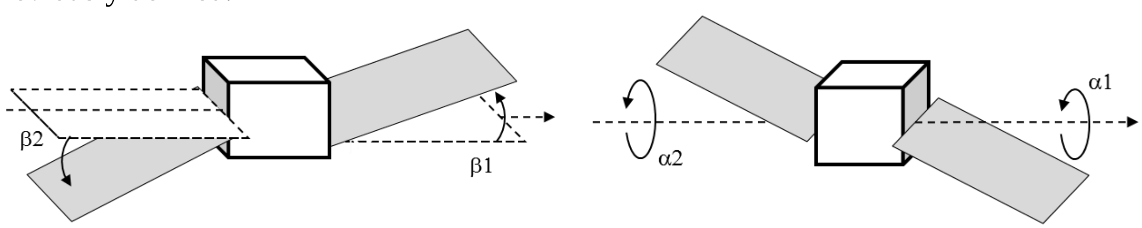

Figure 4. Tilt and rotation angles of the solar panels

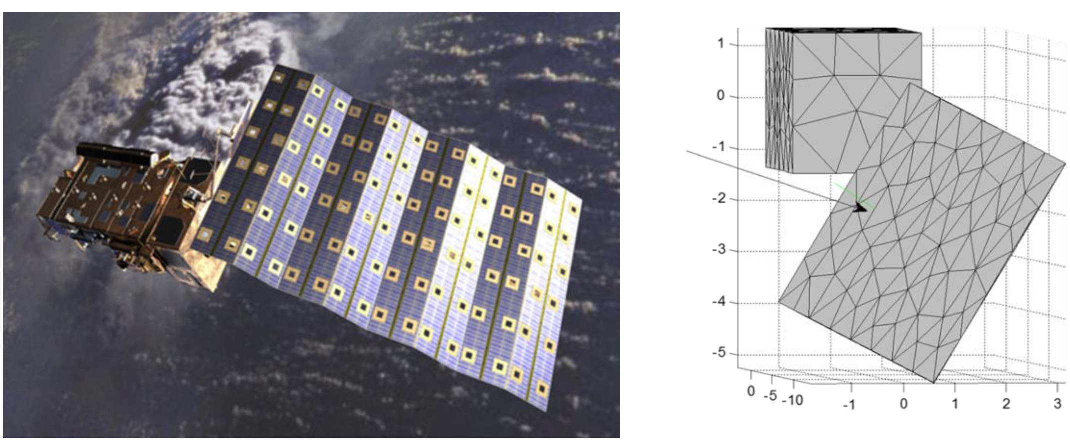

Figure 5. Metop spacecraft and correspondent AADD detailed mesh definition

Given the parameterization of the central body and the solar panel(s) a function automatically builds the prism and surfaces to mesh the spacecraft body. This approach simplifies the definition of the spacecraft and allows a mechanism to automatically modify the spacecraft as function of its parameters (see the Metop mesh definition in Figure 5).

5.2. Orbit history input

The AADD tool doesn't perform orbit propagation, but it pre-load an orbit history generated, from a VisualFocus input file (commercial software from GMV used by EUMETSAT for 3D orbit/attitude visualizations), as ECI(J2000) time-stamped list of state vectors (position,velocity).
The orbit file is pre-processed and stored in a Matlab binary file (.mat) file which is then fed to the simulator. To allow different step sizes, an interpolation is included that computes a Keplerian propagation in the instants in between samples of the orbit file.
To smooth the interpolation, in fact it is carried a forward (from t0 to t1) and a backward interpolation (from t1 to t0), and both contributions are weighted by the proximity to t0 and t1:

5.3. Attitude laws

The attitude laws allow for cumulative construction, and they are listed below, with the possible combinations:

- Local orbital geocentric frame attitude (body-fixed frame with one axis pointing to Earth centre and a second axis pointing towards the orbit normal)
- Local orbital geocentric frame attitude with yaw steering law (body-fixed frame with one axis pointing to Earth centre and a second axis parallel to the ground-track)
- Local orbital geodetic frame attitude (body-fixed frame with one axis pointing to the local normal of the reference WGS84 ellipsoid, and a second axis pointing towards the orbit normal)
- Local orbital geodetic frame attitude with yaw steering law (body-fixed frame with one axis pointing to the local normal of the reference WGS84 ellipsoid, and a second axis parallel to the ground-track)
- Earth target pointing attitude (body frame pointing to a fixed point on the Earth surface and second axis as close as possible to the instantaneous orbital velocity or to the Earth rotation axis)
- Fixed inertial pointing attitude (for single spin stabilised spacecrafts)

Additionally, the attitude bias programming allows defining any kind of attitude manoeuvres on top of the available target pointing above.

5.4. Solar panel rotation laws

Two solar panel laws are applicable. The solar panels rotate with a constant rate $\dot{\alpha}$ or to maximize the sun exposure. No dynamics is considered and discontinuities in the rotation angle are allowed.

- Constant angle: In this case the solar panel angles are constant
- Constant rate: In this case the solar panel angles evolve with the law with fixed rates given by constants and the sampling time. The attitude rates may be considered different for both panels.
- Maximum exposure: In this case the rotation angles of the solar panels are chosen to maximize the direction to the Sun.

5.5. On-line computation of Inertia and Centre of Mass

According the usage of thrusters (depleting mass) and the movements of the solar array, the total mass properties of the spacecraft are re-computed at each step of the simulation.
The computation of the total inertia is done using the Huygens-Steiner theorem, summing up the contribution of the central body and the solar array(s)

5.6. Earth/Moon eclipses and Moon phase computation

While orbiting Earth, the visibility of the Sun from the spacecraft will eventually be blocked. The eclipse of the Sun can be detected by checking the line of sight of the spacecraft to the Sun, where an eclipse occurs if the distance of the Earth's surface to the line of sight vector is less than its radius. The eclipse computation considers the celestial body as spherical. This approach assumes the simplifications:

- the non-sphericity of the Earth is not considered (that could be introduced to replace Earth's radius)
- refraction models of the beam in the atmosphere are not considered.

For the Moon the same algorithm can be applied; the eclipse conditions are given as logical OR between Earth and Moon eclipses. For Star-Tracker related analysis, the tool also computes the Moon phase as seen from the spacecraft.

5.7. Disturbances computation

The disturbances modelled in the AADD-tool include:

- Gravity gradient
- Magnetic
- Solar radiation pressure
- Aerodynamic

The following table shows the compliance of the implementation with respect to ECSS, summarising the consistency between the implementation of the effects and the ECSS standards. The main effects stated in requirements for Space Environment (gravity gradient, magnetic field, solar radiation and atmosphere) only differ to the ECSS for the wind model, anyway not required for the tool, where a simplified model was assumed, where the atmosphere is fixed to Earth.
The ephemerid is also accordingly to the DE405 JPL databases, as defined in the standard.
Two other effects are taken into account, and are not specified in the ECSS: shadowing and shear stress. These two effects will impact the disturbances results since the former changes the effective area, and the latter introduces spurious tangential components to the disturbances forces (and consequent torques).

Both the sun pressure and atmospheric disturbance computation depend on the geometry of the spacecraft and the respective tiles. In the case of the tool, the solar panel(s) rotate changing the geometry along the simulation. The mesh is updated at every simulation step, when the relative position of the tiles of the solar panels is updated accordingly to the commanded solar panel angles.

Table 1. Summary of compliance of the implementation with respect to ECSS

Effect	ECSS-E-ST-10-04C	ACTION
Solar radiation model	Compliant with standard	-
Atmosphere model	Compliant with standard	NRLMSISE-00 model implemented (suing MSFC bulletins). JB2006 model not required.
Magnetic field model	Compliant with standard	IGRF-10 model implemented.
Gravity gradient	Not addressed in ECSS	Model implemented compliant with literature see [3], without considering geopotential effects (Earth as point mass)
Magnetic	Not addressed in ECSS	Model implemented compliant with literature, see [3], SC modeled as single dipole
Solar radiation pressure	Not addressed in ECSS	Model implemented compliant with literature , see [3], using 3D mesh model
Aerodynamic	Not addressed in ECSS	Model implemented compliant with literature, see [3], using 3D mesh model
Wind model	Not compliant with standard	Not required. Simple model implemented. Atmosphere fixed with the Earth.
Shadowing	Not addressed in ECSS	Model inherited from previously implemented libraries.
Shear stress	Not addressed in ECSS	Model inherited from previously implemented libraries.
Planetary Ephemerides	Compliant with standard	DE405 JPL ephemerides implemented.

It is also noted that the aerodynamic model is quite sophisticated, thanks to its heritage from dedicated studies for the ESA (very) low-earth orbit mission GOCE (down to 250 km altitude). The aerodynamic drag acceleration is computed (according to the implemented relative wind model) using the model of Schaaf and Chambre. This is a modification of the Maxwell model introducing the accommodation coefficients, so that the pressure and shear stress are computed with a different participation of specular reflection. The introduction of an additional parameter improves the accuracy of the model.
To calculate the forces upon a surface element, the momentum transfer in normal and tangential directions are evaluated.

5.8. Reaction Wheels de-saturation analysis

The momentum wheels absorb disturbances acting on the satellite and without a de-saturation scheme they would eventually reach their saturation limit. If this happened, they would no longer be able to maintain a stable attitude of the satellite. To avoid this, angular momentum must be moved from the satellite to the inertial system, by applying an external torque with the magnetorquers or thrusters. The process is shown in Figure 6. It is decomposed into 5 sub-processes (A1 to A5), each can be configured through parameters by the user, that will be briefly introduced in the following text.

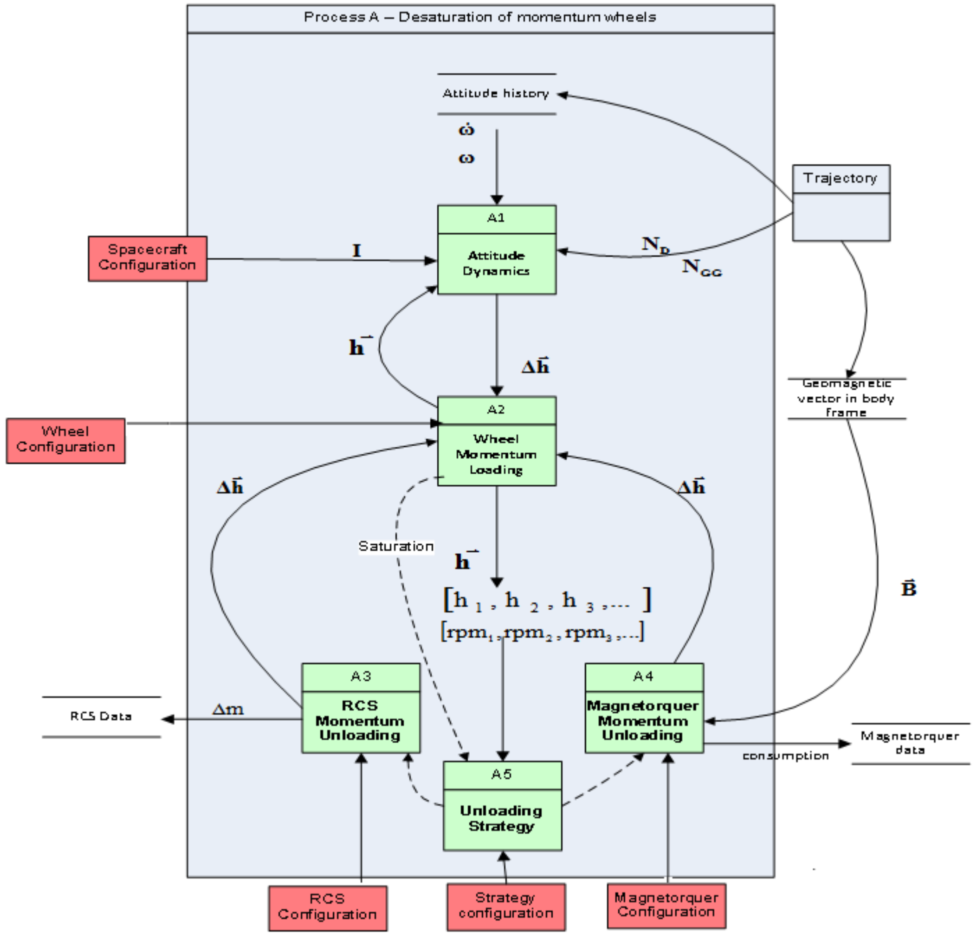

Figure 6. Reaction Wheels, Momentum De-saturation process

<u>A1 Attitude Dynamics</u>: The attitude dynamics block receives attitude / torques history data and computes the momentum loaded to the reaction wheels due to external disturbances (not including magnetorquers/RCS commands). The attitude dynamics are modelled using the Euler equation with reaction wheels (see [3]). The stored momentum is computed by integrating this in time with no contribution of the actuators, and solved for $\dot{\mathbf{h}}$; For a time frame of Δt the extra momentum that is to be loaded to the reaction wheels due to the dynamics is $\Delta\mathbf{h} = \Delta t\dot{\mathbf{h}}$.

<u>A2 Wheels Momentum loading from space environment</u>: the accumulated momentum $\mathbf{h}$ is tracked in A2. It receives the contributions in the time frame Δt to changes in angular momentum $\Delta\mathbf{h}$ and computes its distribution among the momentum wheels. The parameters for this process are the wheel system configuration.

- Reaction wheel steering law: It is assumed that for a time instant the total sum of additional angular momentum loaded (or unloaded) into the wheels is distributed pseudo-inverse of the wheels mounting matrix
- Reaction wheel steering law during de-saturation: here the steering law follows limitations for gradual de-saturation imposed by the user.

  Wheel saturation: To keep track of this, the parameters used are the inertia of a wheel, the maximum rotation for a wheel or the maximum angular momentum accumulated in a wheel.

The wheel momentum loading process keeps track of the momentum/speed of each reaction wheel so that information of saturation can be provided to the unloading manager (A5).

A3 RCS Momentum Unloading: the RCS angular momentum unloading process is activated by the unloading strategy manager (A5) and provides the $\Delta\mathbf{h}$ of unloading momentum from the RCS to the wheel momentum loading process (A2). Furthermore it computes the ejected mass for computation of the propellant consumption. It uses as input the direction of the thrusters (as a parameter). The RCS angular momentum unloading is based on MTG (proprietary) code. The following limitations are applied to thrusters behaviour: Minimum Impulse Bit (if the required change in momentum per thruster is lower than an input value, then the thrusters' valve is considered not to open), and Maximum thrust (saturation)

A4 Magnetorquers Momentum unloading: the magnetorquers angular momentum unloading process is activated by the unloading strategy manager (A5) and provides the unloading delta momentum from the magnetorquers assembly to the wheel momentum loading process (A2). Furthermore it computes the consumed power. The magnetorquers can be used to unload momentum, in the direction of the component of loaded angular momentum that is perpendicular to the geomagnetic field. The effect of magnetometer sensing accuracy is also modelled.

A5 Unloading Strategy: the unloading manager tracks the accumulated momentum in each wheel and, according to user settings, manages the magnetorquers and the Reaction Control System (RCS) unloading activations to dump wheel momentum. It sends the commands of required to RCS (A3) and Magnetorquers (A4) process. The strategies are the following, and can be set in combination (that is, any of the strategies can be turned on or off).

Magnetorquers angular momentum dumping

- Continuous unloading – the Magnetorquers process (A4) is commanded to try to cancel (at its maximum capability) at all times, the component of the loaded angular momentum in the direction perpendicular to the magnetic dipole
- A threshold can be to avoid using the magnetorquers when the angular momentum to unload is near the geomagnetic vector direction
- A threshold can be set to only activate the magnetorquers if any of the wheels is above that

RCS angular momentum dumping

- Unload periodically – in this case the manager activate the RCS to dump the momentum at a predefined rate. It will call the A3 process in periods set by user.
- Threshold for angular momentum. In this case, A3 will be activated upon a threshold and the manager will keep track of the number and instant of firings, with an alternative dump of momentum upon reaching a maximum accumulated momentum threshold, or when reaching a maximum accumulated momentum or rpm in one wheel
- Dump total momentum – in this case the RCS is informed to unload the total momentum.
- Dump momentum of one wheel– in this case the RCS is informed to unload the momentum of a single wheel (the one that reached saturation). A3 is informed to unload where is the momentum (in body frame) of the saturated wheel

- Dump to bias rate of the wheels – in this case the RCS is commanded to unload in a way that the wheels will be offloaded to a given required angular velocity.

Combined RCS and Magnetorquers angular momentum dumping

- This mode can drive the combined usage of RCS and magnetorquers, as described above

5.9. Instrument blinding/occultation analysis

The analysis of the Instrument blinding/occultation is of particular interest for EUMETSAT spacecraft, both for investigation of mis-performances (as when the instrument is a Star Tracker and the Sun/Moon/Earth appears in the field of view) or potential calibration (for optical payload, the Moon is used for in-flight calibrations). This analysis is based on geometric ray tracing between the instrument (considering the angles of the sensor visibility cone) and the different objects that may cause occlusion, Sun, Moon and Earth. When occlusion/blinding occurs, flags should be activated stating the source object.

Stated below is the algorithm for the Moon, but it is valid for any celestial body.

- The relative vector between the spacecraft and the Moon is computed. The relative vector is rotated into the body frame using the attitude of the spacecraft. The angle between the instrument bore-sight and the Moon relative position is computed using the internal product with the relative position vector, but also considering elliptical field-of-view of the sensor. The angle from the Moon's limb cone is computed based on the Moon radius as seen from the spacecraft and the relative distance of the spacecraft with respect to the Moon centre.
- This angle is compared with the Instrument exclusion angle for the Moon and the angle of the Moon limb angle, to see if there is a cone intrusion (where the two cones intersect).The exclusion angle specific to the Moon (from configuration parameters) determines how much can the Moon cross into the visibility cone without causing blinding. Different exclusion angles are specified for the Sun and Earth. To disambiguate the direction where the Instrument is facing, the relative position direction is projected on the Instrument direction (positive if Moon relative and Instrument are in the same direction).
- Phase of the Moon and Earth are also included, where thresholds are defined for these two celestial bodies above which the illumination becomes relevant for the blinding decision.
- The final condition is if the Moon is behind the Earth. In this case, the blinding is to be ignored.
- If all conditions are fulfilled, then the Moon is causing a Instrument blinding.
- The blinding is flagged every time a blinding/occultation of one of the celestial bodies occurs: $Moon\ blinding \vee Earth\,blinding \vee Sun\ blinding \Rightarrow STblinding$

It is assumed here that the Instrument cone is not blinded by elements of the spacecraft itself.

Also, the Instrument location in the geometric body frame is not considered, and it is approximated by the Spacecraft reference frame origin.

Not all of the conditions are applicable to all of the bodies: the cone intrusion is checked for all bodies, the phase is checked only for Earth and Moon blinding, while the Earth occultation only for Sun and Moon. The tool foresees the configuration of up to 3 star-trackers. The analyses obtainable by this functionality are applicable for any sensor with conical field of view (with circular or elliptical section).

5.10. Solar power estimation

The power supplied by the solar arrays can be estimated from the Solar radiation angle on the panels. The same information used to evaluate the solar exposure to solar pressure can be used to estimate the power supply.
The maximum power will be available when the sun line is normal to the array. A trigonometric relationship can be found between the sun incidence angle γ and the power available: $P_{available} = \cos(\gamma) P_{\max}$. Typically this holds up to 60 degrees, after which it is no longer representative. When the incidence starts getting parallel to the solar array surface, effects like finite thickness of the cells and specular reflection from the cover glass surface, break this relationship. The selected function is , and, with $\frac{P_{available}}{P_{\max}} = area * power_{ratio}$, with the power ratio equal to 0 if in eclipse or for γ < -π/3 or γ >+π/3, equal to cos(1.5 γ) otherwise, where 1.5 is the ratio of , (π/2)/(π/3)so that the function reaches null at 60 degrees.
The incidence angle of the solar panels and illuminated surface is retrieved from the shadowing analysis and solar pressure analysis. In the sun pressure computation, the illumination and incidence angle is evaluated for each one of the tiles that compose the spacecraft mesh.
The incidence angle is evaluated using the internal product between the sun incidence direction (taken geometrically from the position and attitude of the spacecraft) and the norm vector of each of the tiles. The incidence angle is taken as the mean incidence angles for all the illuminated tiles. This approach also allows the use of the shadowing analysis (to remove shadowed areas of the solar panels) and provides a better estimation of the illuminated area for power supply computation.

7. AADD tool verification & validation

The different supporting AADD tool models have been validated by comparison with provided reference validation data:

- For the case of models re-used from previous validated tools, the reference validation data are produced by using the original validated models.
- For the case of newly developed models, reference validation data are searched in the available literature, provided by independent software/simulation tool, or compared directly with flight data

The independent software tools for validation include STK, NAPEOS, Simulink Aeropsace Blockset. Reference data are taken from the simulation campaign run for validation of the AOCS design by the spacecraft manufacturer. Flight data are taken from the EUMETSAT operated satellites, principally MSG and Metop.
The final test campaign foresaw a total of 42 unit test (breaking down the single functionality of the tool) and 10 system tests.

As an example, this paper shows the results of one of the more complex system validation tests: Guidance/Desaturation LEO. This test foresaw the validation of different components of the AADD tool: Attitude guidance (geodetic with yaw steering), the disturbance model (All), the correspondent wheel loading and the de-saturation scheme with continuous off-loading using exclusively magnetorquers. The reference data for this test were taken directly from the

telemetry of Metop, reporting the wheel speed evolution in-flight while continuous that operates in similar conditions. The test preparation took into account a synchronisation of all simulation parameters (guidance parameters, mass properties, geometry, solar array rotation, thermo-optical properties, actuators parameters, both for magnetorquers and 3 active wheels, etc..) as well as the use of the actual orbit, as determined on-ground by the control centre, in the period of the reference telemetred data. The comparison of the wheels speed as simulated by AADD with the correspondent values coming from Metop telemetry is shown in Figure 7: this shows an excellent agreement that resulted in the test to be successfully passed.
It is noted that this results could be even further improved with fine tuning of the assumed simulation model for the spacecraft residual dipole (in magnitude and direction) that is not known on-ground for Metop, and also modifying the default thermo-optical properties, to take into account aging of materials. A sensitivity analysis is currently on-going to further improve these results.

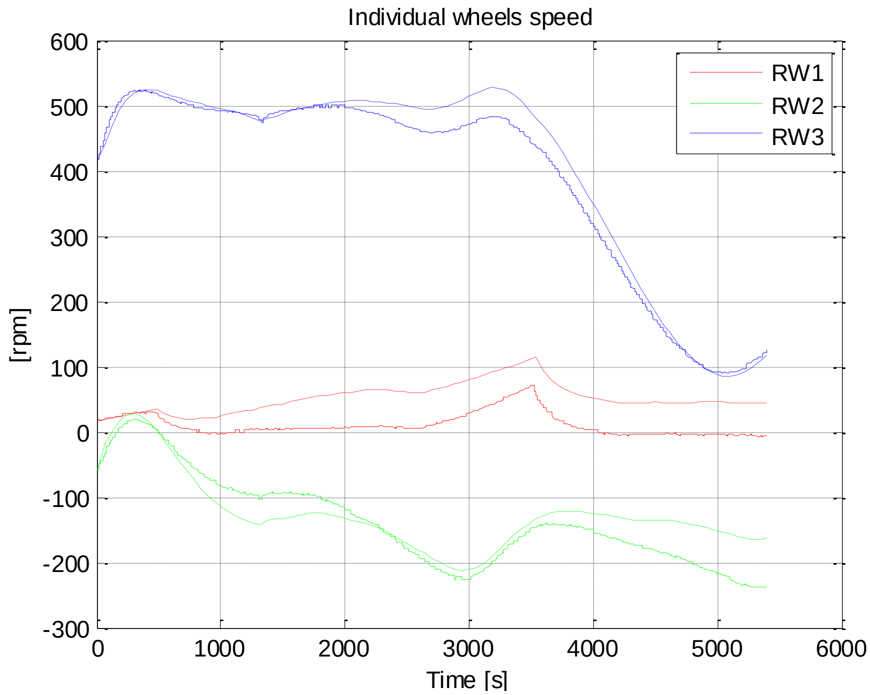

Figure 7: Validation of Simulated reaction wheels speed vs. Metop Telemetry flight data

8. LEO study case results

The scenario for this study case is described hereafter:

- Three-axis stabilised spacecraft in the LEO orbital environment.
- Earth Geodetic Yaw Steering attitude law.
- One rotating solar array, maximizing sun exposure
- Star trackers for pointing estimation, with 3 wheels and 1 magnetorquer for attitude control and wheel de-saturation respectively.

The base spacecraft is Metop, with a central body and a single solar panel (Figure 8 for the assumed mesh for the frame definition; to be noted that this is a simplified version of Figure 5, for speeding up the simulation execution, to the known missing shadowing).
No star trackers mounted on Metop. For the purpose of the analysis of Instrument blinding/occultation, a set of star trackers was added based on the Sentinel-3 star tracker setup, fixed in Geometric centre.
The STR alignments are actually taken from Sentinel-3, taking care of the different definition of the body from Sentinel-3 frame to Metop frame.
The desaturation uses continuously the magnetorquers.

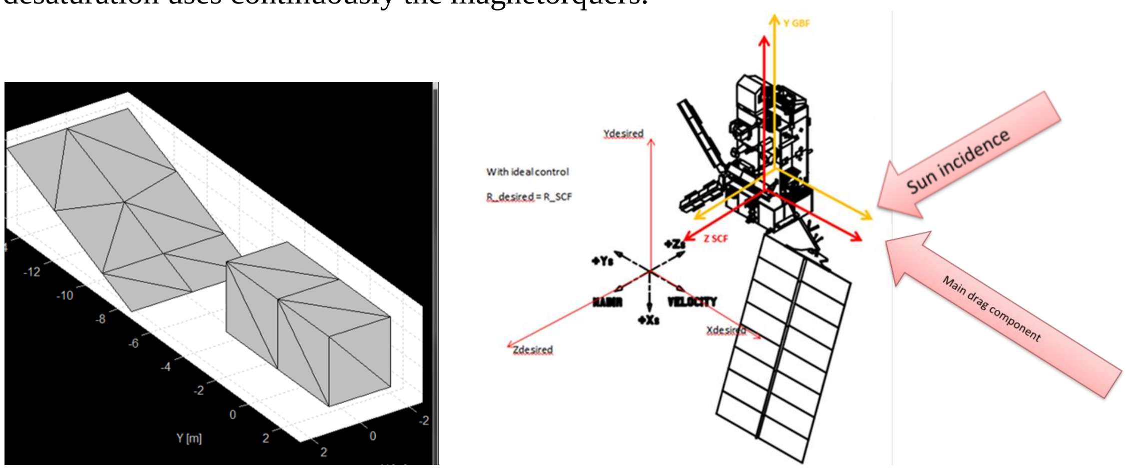

Figure 8: Metop reference frames for LEO study case

For this study, 2 LEO orbit files are used, each of them assuming a different level of solar activity (50% or 95% percentile on F10.7 solar radio flux from MSFC bulletins, respectively labelled as mean or high solar activity), thus giving 4 simulation cases; The first scenario is based on Metop routine-operations reference orbit (sun-synchronous with 29-days repeat cycle) while the second in an eccentric re-entry orbit case (800x600 km altitude).
LEO Setup-1 and Setup-2 are respectively based on Routine orbit with mean/high solar activity.
LEO Setup-3 and Setup-4 are respectively based on Re-entry orbit with mean/high solar activity.

This paper is not meant to be exhaustive of the study results, but of the possible analyses. Therefore, the full modelling parameters will not be given, and only the results related to LEO Setup-1 will be shown (see [4] for full details about modelling parameters and results).

The results related to the torque disturbances are presented first (see Figure 9, Figure 10, Figure 11 and Figure 12).

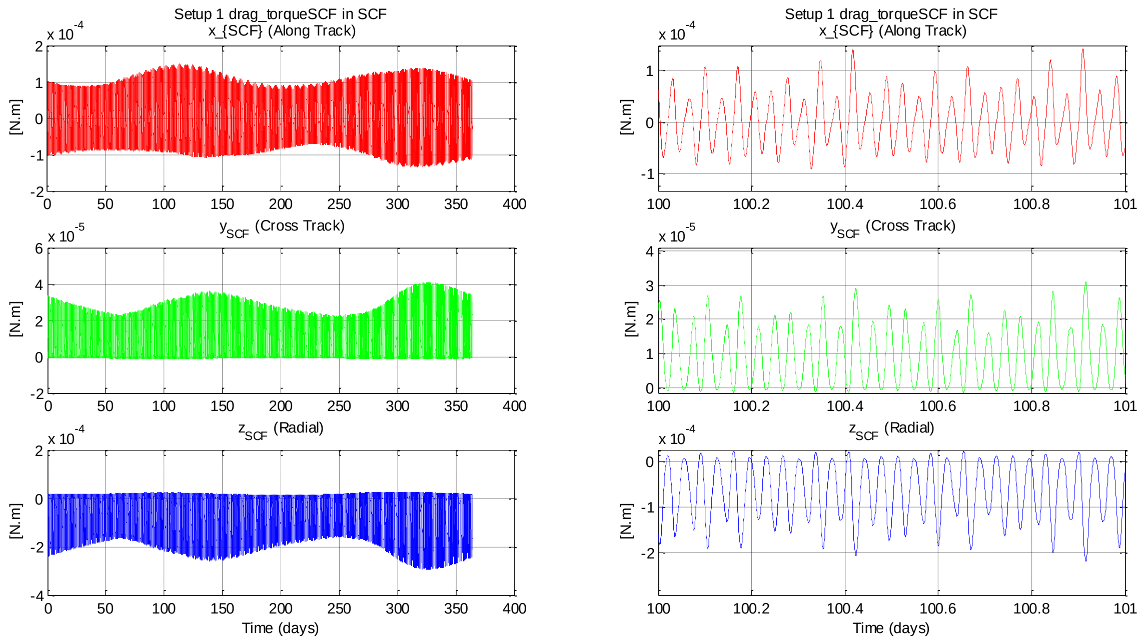

Figure 9. Drag torque history, 1 year (left) and zoom on 1 day (right)

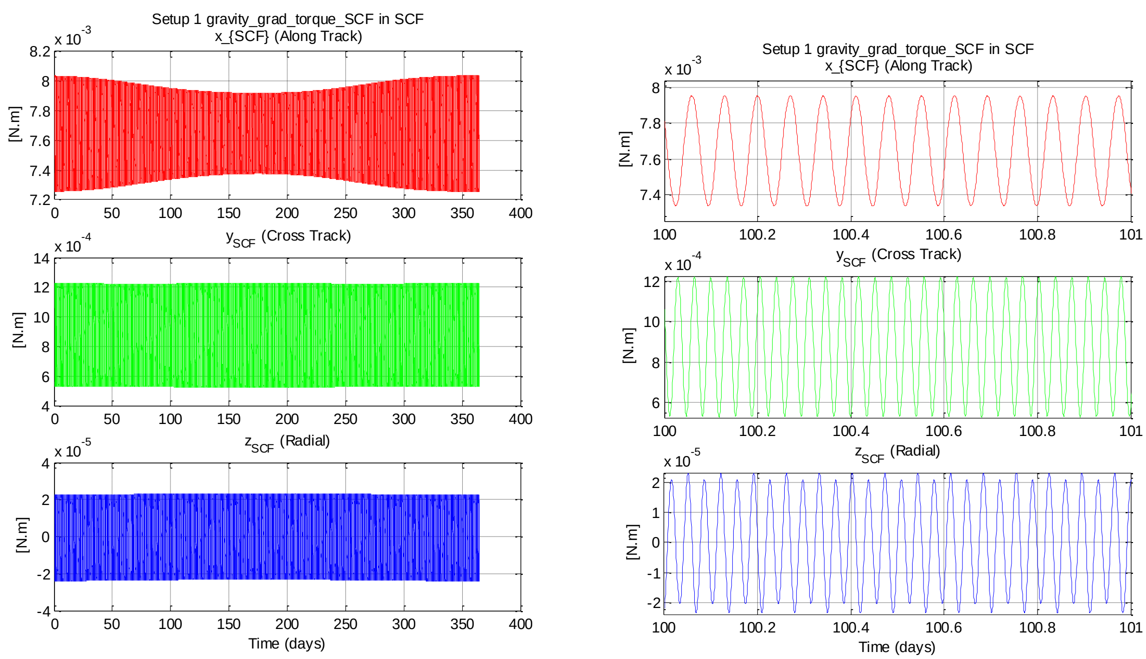

Figure 10. Gravity gradient torque, 1 year (left) and zoom on 1 day (right)

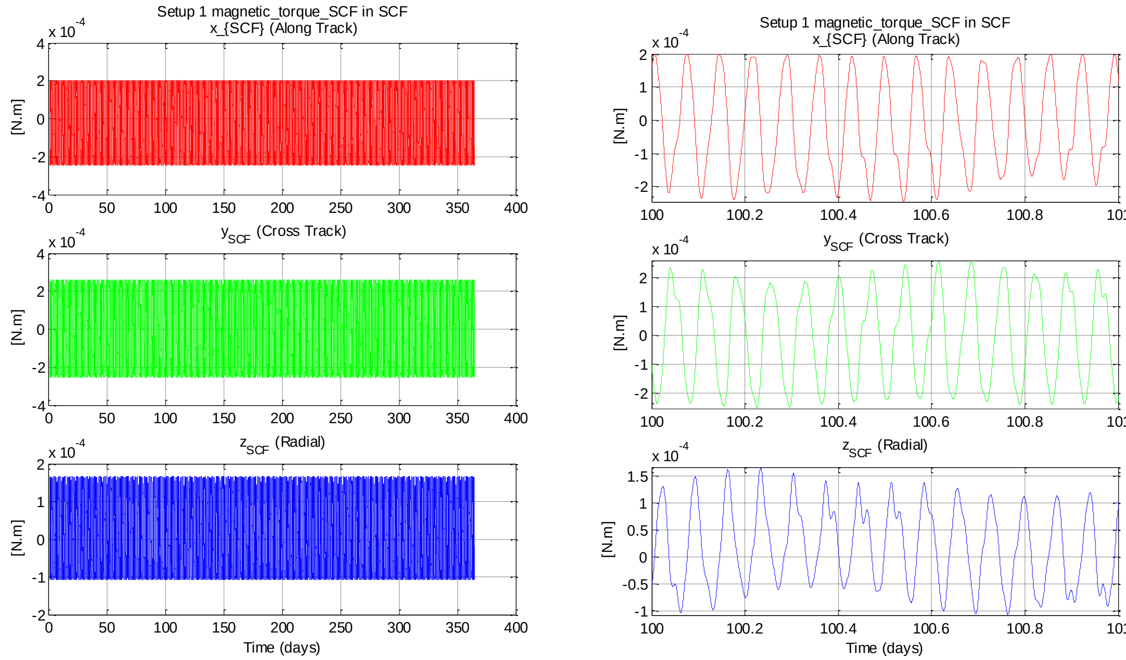

Figure 11. Magnetic torque, 1 year (left) and zoom on 1 day (right)

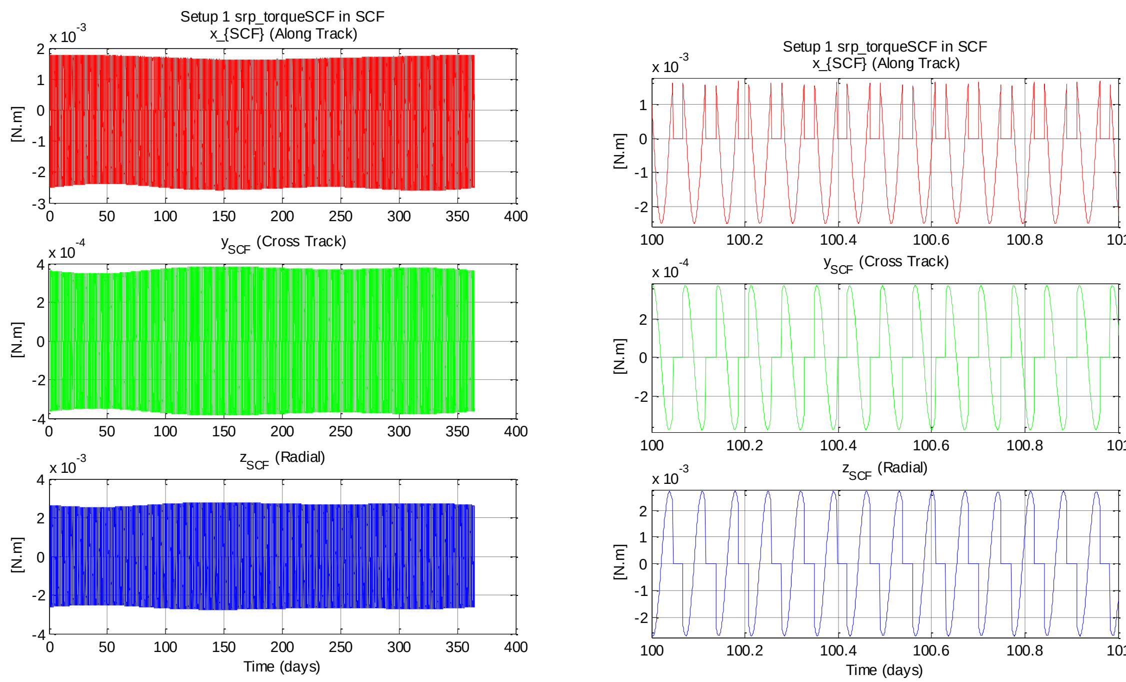

Figure 12. Solar Radiation Pressure torque, 1 year (left) and zoom on 1 day (right)

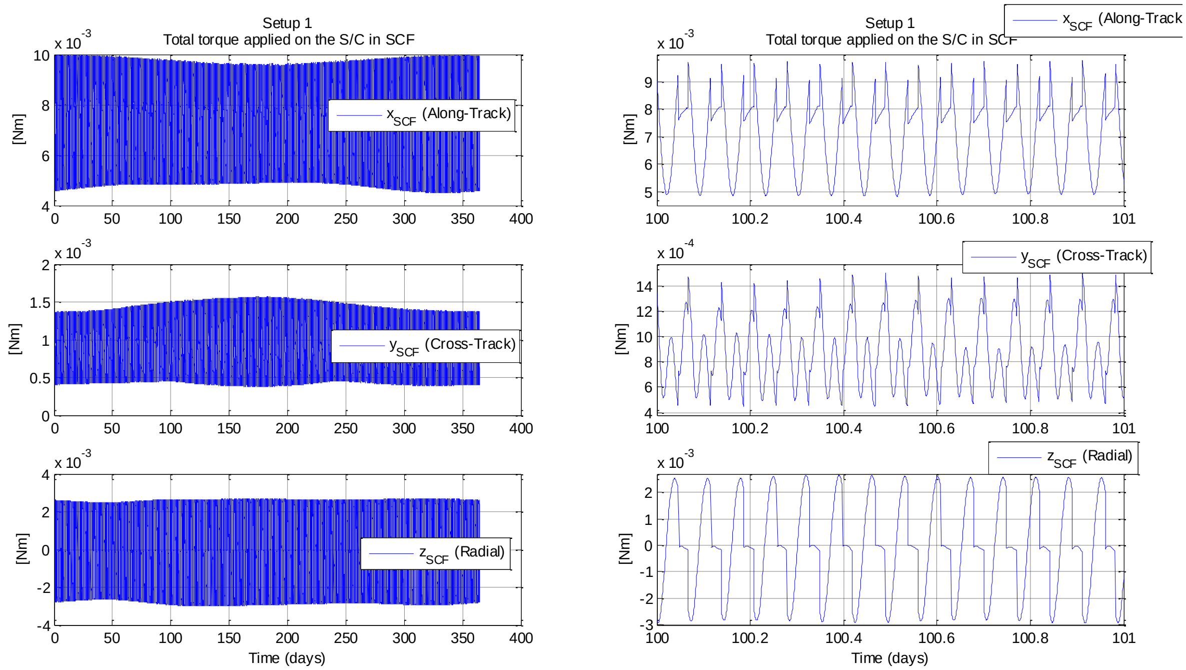

Figure 13. Total torque, 1 year (left) and zoom on 1 day (right)

The conclusions (see Figure 13) for this analysis are that:

- There are bias components in X_SCF and Y_SCF
- That Z_SCF contributes with significant torque but with small mean value
- In both setups, overall, the impact of MSFC is not noticeable since most of the contributions are: Gravity gradient in X_SCF and Y_SCF (followed by some solar radiation pressure torque); Solar radiation pressure in Z_SCF (followed by some drag and magnetic torque)

In the loading history of the wheels (that are aligned with the body axis), it is possible to see that they are capable of storing the needed torque (see **Figure 14**).

In all the cases, there is a bias in the loading on the second wheel related to the gravity gradient torque bias in X_SCF. The maximum amplitude is the third wheel related with Z_SCF (although with a smaller mean value).

During most of the history, the μ vector generated by the magnetorquers is close to the maximum allowed, **Figure 15**. During some periods it is actually saturated, however without any risk of reaching saturation of the wheels.

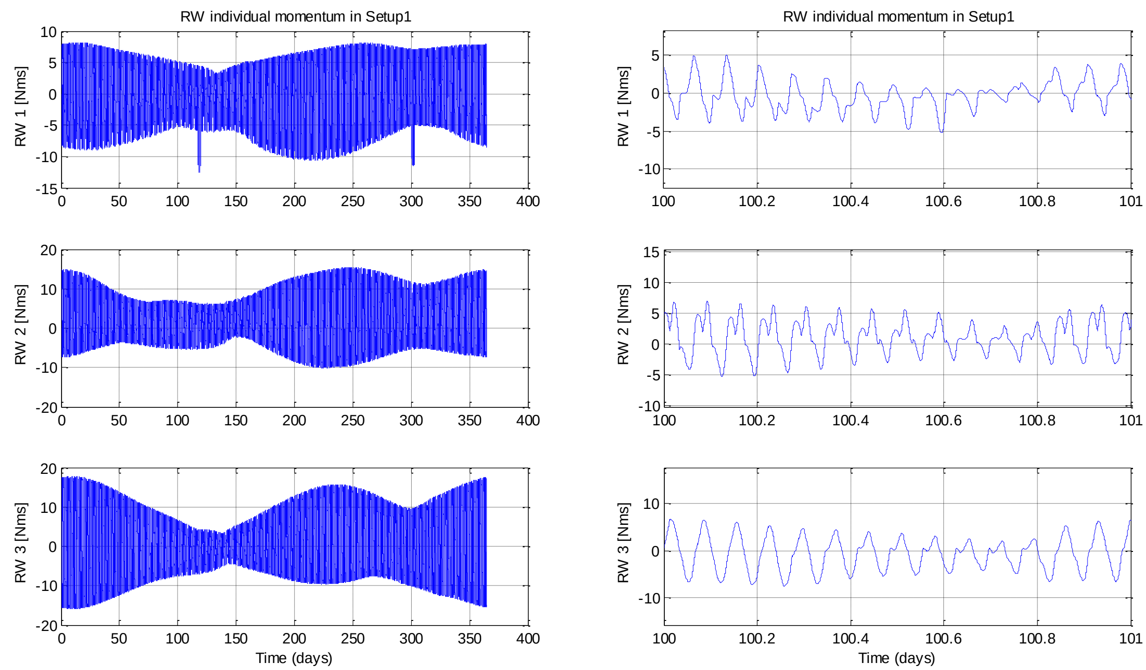

Figure 14. Moment loaded in each wheel (left) and detail about 1 day (right)

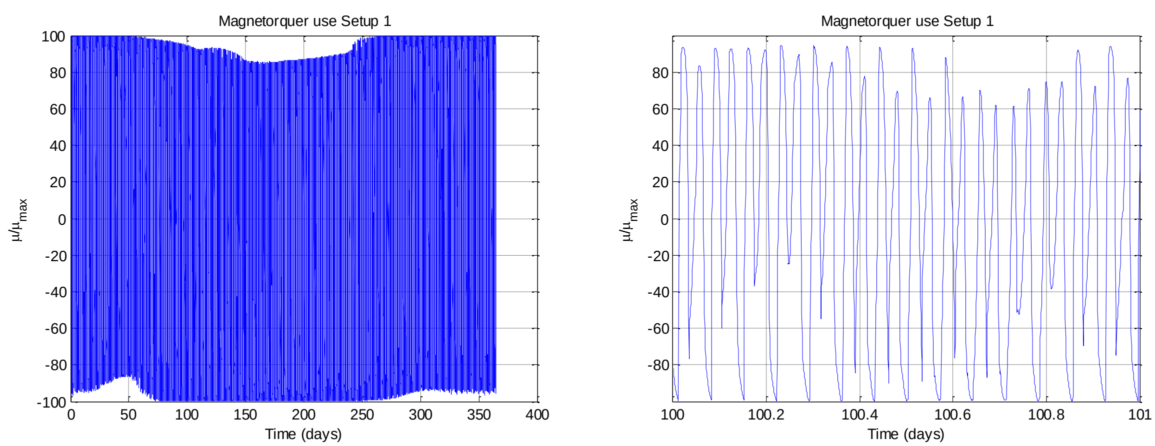

Figure 15. Percentage of magnetorquer capacity use (μ / μmax) (left) and detail about 1 day

Related to the Startrackers analysis Figure 16 shows that all the occurring blinding of the star trackers are caused by the Moon, that the angle between the Sun and the exclusion angle has a margin over 25 degrees, while the Earth (not shown) maintains almost constant angle to boresight with respect to the star trackers, as expect from the Earth-pointing guidance profile.

The power supply is affected by the eclipses that in this case are very frequent, while one can plot the available power without the instances where it is null due to eclipses (see **Figure 17**).
From the latter it is possible to see that, excluding the eclipse moments, the power supply availability is always above 80%. The tool also allows estimating the effect of the less frequent Moon eclipses.

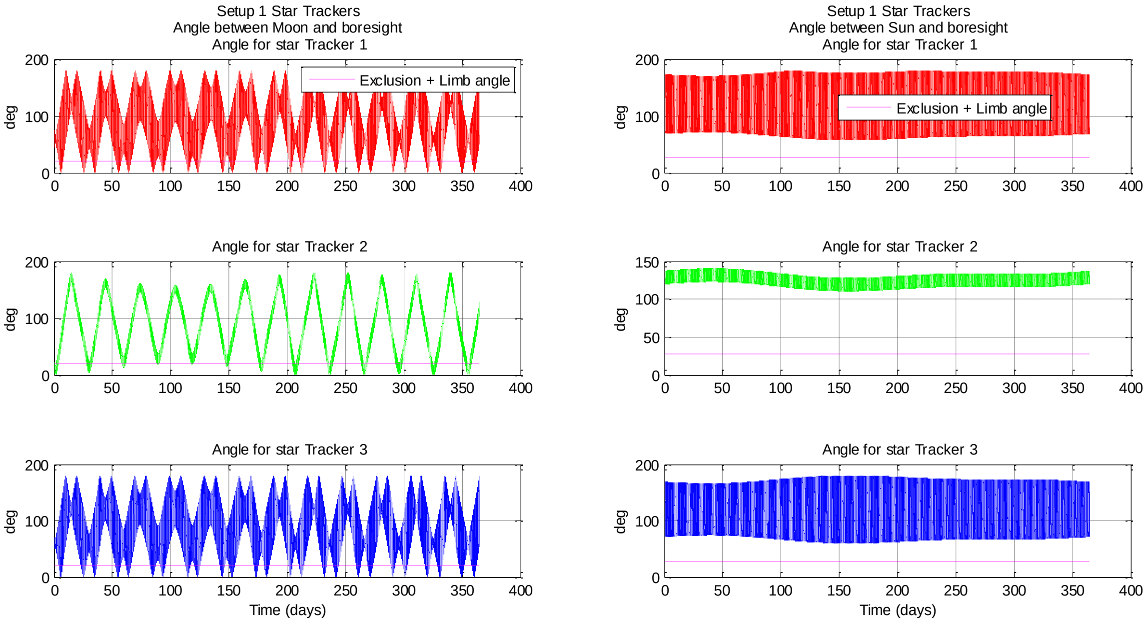

Figure 16. Angle between boresight vs. Moon (left) and vs. Sun (right)

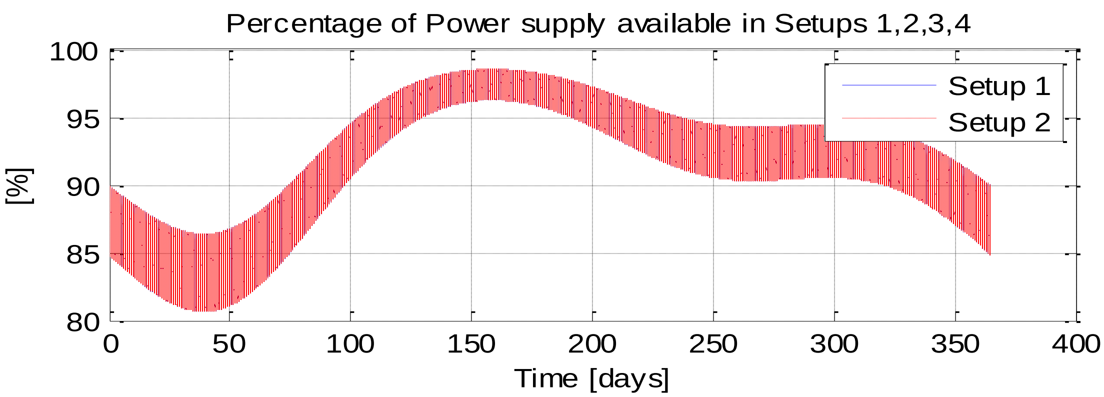

Figure 17. Percentage of available power supply , when excluding the eclipse

9. GEO study case results

The scenario for this study case is described hereafter:

- A three-axis stabilised spacecraft in the GEO (or GTO) orbital environment.
- Attitude law to fixed point on Earth surface, and scheduled yaw flip manoeuvres (180 degree yaw rotation every 6 months, at equinox).
- 2 sun-facing rotating solar arrays (at constant speed).
- Star trackers for pointing estimation, and 5 wheels and 4 thrusters as actuators for attitude control and wheel de-saturation respectively.

The base spacecraft is MTG (Meteosat Third Generation), with a central body and double solar panels (see Figure 18 for the assumed mesh and for the frame definition).
The simulation of the Star trackers is based on the MTG current configuration of the sensors.
The wheels' de-saturation uses the thrusters, as from MTG current design (as from spacecraft PDR).

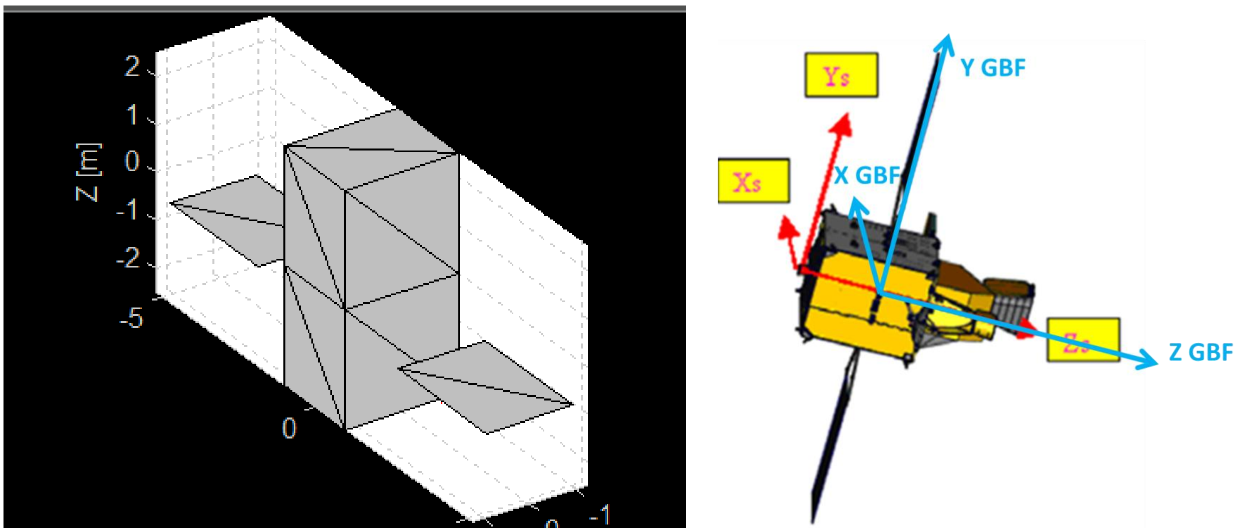

Figure 18: MTG mesh and reference frames for LEO study case

The 3 GEO orbit files for the 4 simulation cases are based on actual station-keeping simulations (0º East/West control with +/-0.1º dead-band, with inclination controlled around 0º (Setup 1) or 1º (Setups 2&3); The 3rd orbit for Setup 4 is actually a sub-synchronous LEOP transfer case (GTO-to-GEO), taken from the real determined orbit during MSG-3LEOP.
Setups 1 and 2 differ in the orbit history, which will affect all the outputs. Setups 2 and 3 differ in the de-saturation strategy (Setup-2 is based on regular de-saturation strategy in time of the wheels, while Setup-3 has a de-saturation scheme based on Maximum angular momentum for a single wheel, when reached triggering unloading of all wheels together). However, the star tracker and illumination analysis are common. Setup 4 is completely different from the other two setups, in the type of orbit, and it also includes the aerodynamic impact in the torque disturbance.
This paper is not meant to be exhaustive of the study results, but of the possible analyses. Therefore, the full modelling parameters will not be given, and only the results related to GEO Setup-3 will be shown (see [5] for full details about modelling parameters and results).
The results related to the torque disturbances are presented first (see Figure 9Figure 19 and Figure 20). To be noted that the drag disturbance is not relevant for the GEO case.

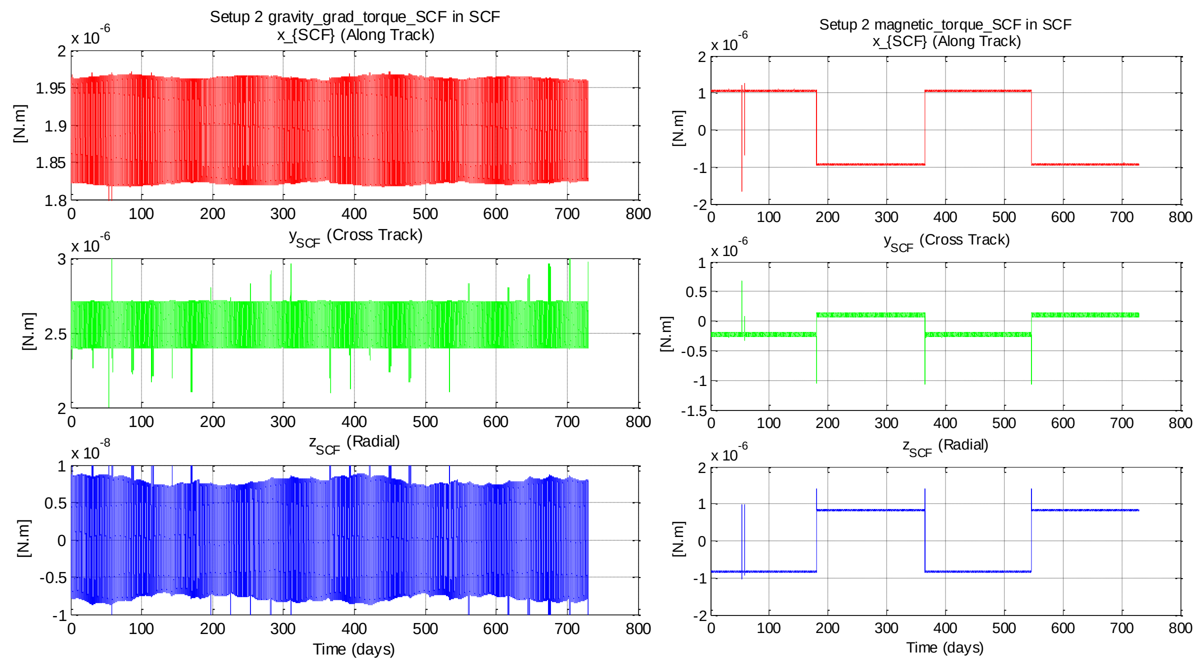

Figure 19. Gravity gradient torque (left) and magnetic torque (right)

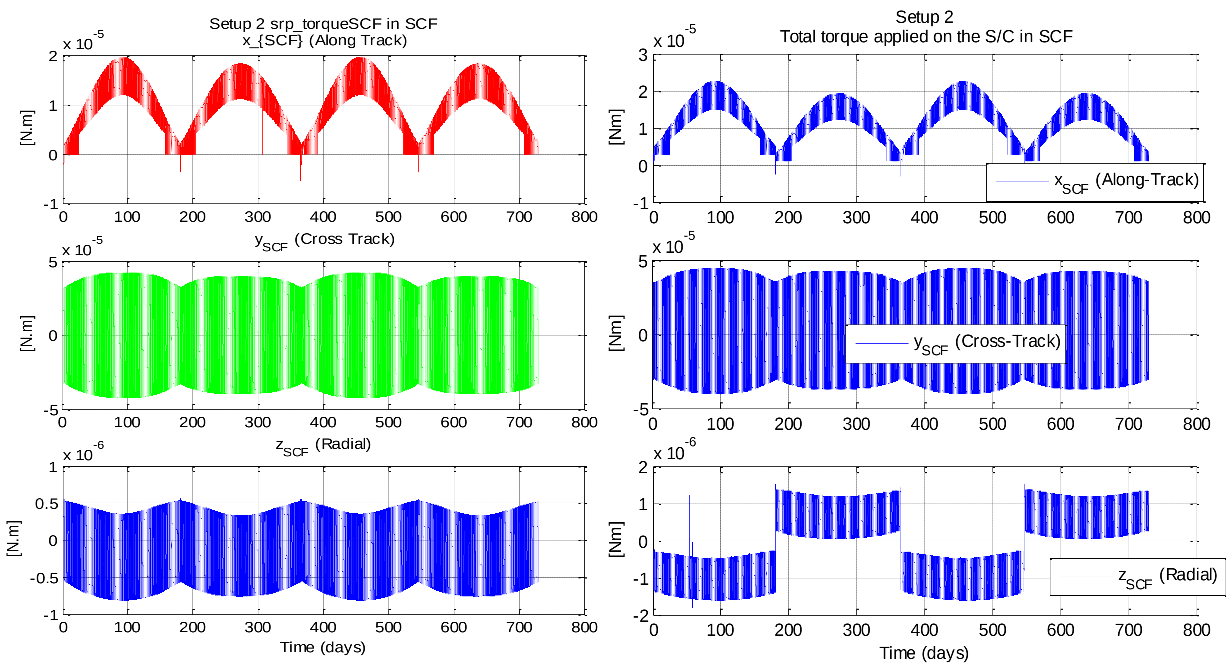

Figure 20. Solar radiation pressure torque (left) and total torque (right)

In the total resulting torque components we have that:

- In X_SCF the solar radiation is dominant, although it is still possible to see the bias introduced by the gravity gradient and the added and subtracted contributions from the magnetic torque (especially at equinox)

- In Y_SCF, the torque is completely dominated by the solar radiation pressure
- In Z_SCF the magnetic torque is the main contributor, despite the clear effects of the solar radiation pressure torque. It is also clear that this components switches with the yaw maneuver and varies during the season.

The loading history of the wheels for Setup-3 is shown in **Figure 21**, together with the total wheels momentum projected in spacecraft axes. The opening time of the thrusters for wheels off-loading is shown in **Figure 22**, together with the induced orbital Delta-V.

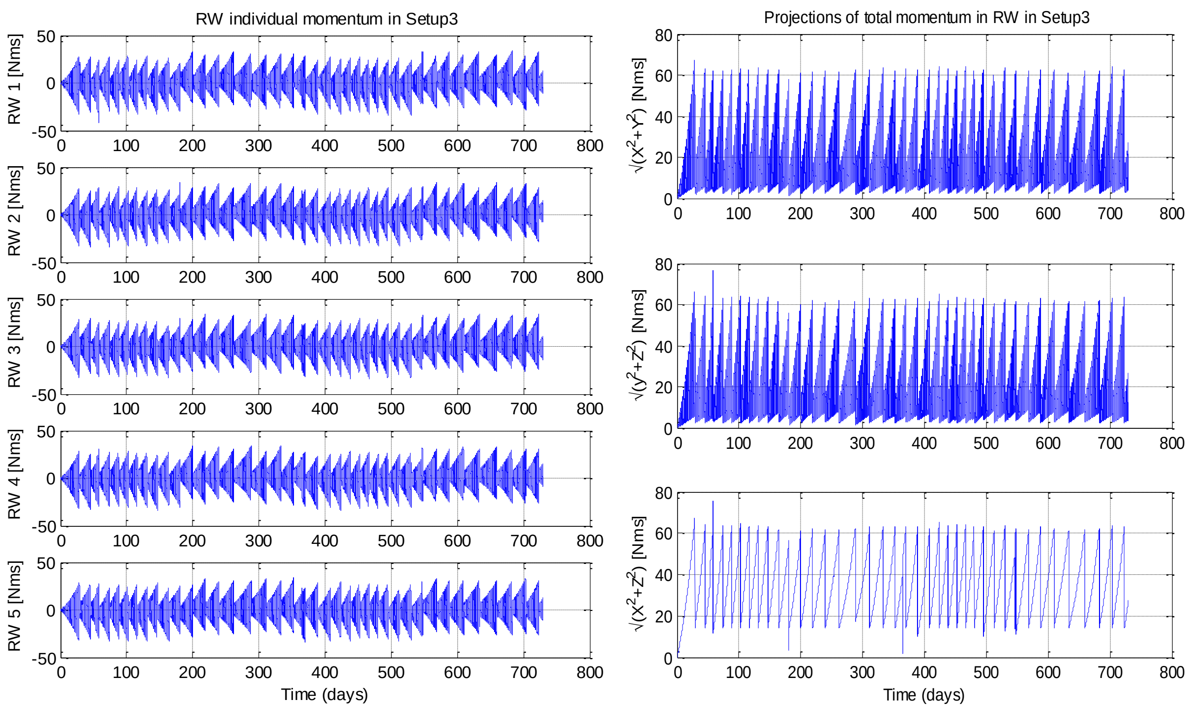

Figure 21. Moment loaded in each wheel (left) and total momentum (right)

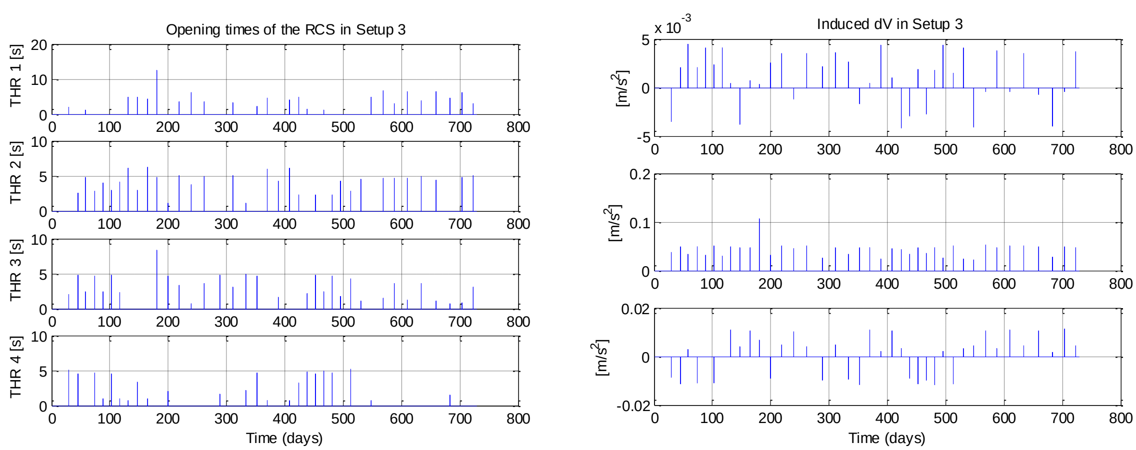

Figure 22. Thrusters' opening times (left) and induced orbital Delta-V (right)

Related to the Star trackers analysis Figure 23 shows that the Sun's blinding is aggregated in sets around a 180 day period. Given the orientation of the Star Trackers and the Attitude guidance, Earth is always outside the exclusion zone (not shown). Both STR 2 and STR3 will be blinded frequently by the Moon and Sun. Both the Moon and the Sun cause long term blinding, with averages going up to 2 hours, and maximum up to 3h20m (12000 sec). For the first STR the Sun has a slightly smaller impact, but still with average blinding of almost 100 minutes.

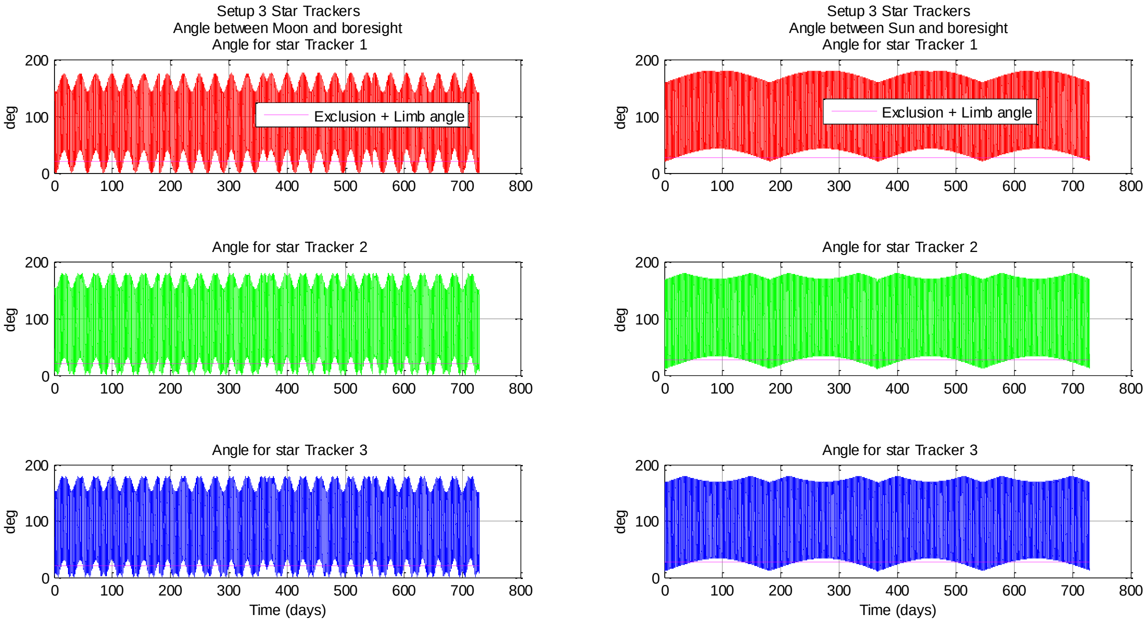

Figure 23. Angle between boresight vs. Moon (left) and vs. Sun (right)

It is possible to see that, due to the incidence angle variations, **Figure 24**, the power supply will oscillate between 80 and 100%. The presence of frequent Earth eclipses that coincide with the best incidence angle, the average power supply will be affected. Despite the frequent eclipses, the average power supply stays close to 90%.

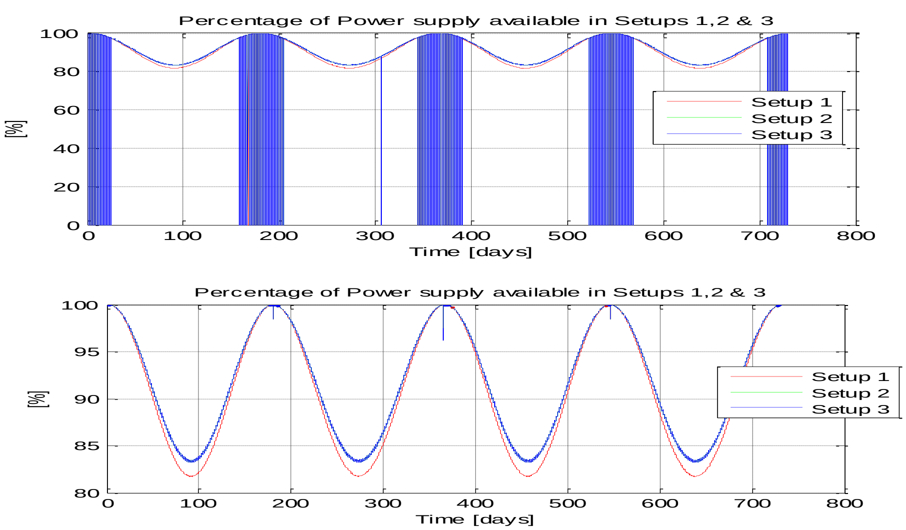

Figure 24. Percentage of available power supply (top), same excluding the eclipse (bottom)

10. Conclusions

EUMETSAT dedicated study called AADD successfully reached the purposed of characterising both for LEO and GEO environment the dynamic loads induced by the space environment, to characterise the wheel off-loading frequency/needs, based on angular momentum accumulation, to predict and analyse the blinding/occultation by Sun/Moon/Earth of instruments (such as star-trackers), together with solar-array(s) illumination.

This has been done for different configurations in both LEO and GEO case, to allow internal sensitivity analysis. This paper reported some of the results as explicative of the adopted process.

The supporting tool developed during this study proved to be very modular and flexible, and it was successfully validated with independent tools and using available flight data as much as possible.

The study is currently being further expanded to cover the simulation of free-dynamics (for long-term attitude analysis of the currently flying satellite, after de-commissioned), the analysis of lunar intrusion in different instruments for evaluating the possibilities of lunar calibration for future missions (i.e. MTG Flexible-Combined-Imager, or EPS-Second-Generation METimage , characterised by different shape of their field-of-view), and for improvement of the analysis of wheels off-loading schemes in support of the Operations-Preparation for MTG.

11. Acknowledgments

This study has been developed by GMV under EUMETSAT guidance and supervision within contract EUM/CO/12/4600001002/Spe .
The authors wish to thank the GMV personnel also involved in the study, S.Ciabuschi, J.Peyrard, J.Branco, E. Di sotto, P. Colmenarejo, for the active and valuable support provided.

12. References

[1] EUMETSAT web-site
www.eumetsat.int

[2] AADD software design document
GMV-EUM-AADD-SDD, Issue 1.5, Date 17/07/2013

[3] Spacecraft Attitude Determination and Control
James Richard Wertz, Springer

[4] AADD Study Cases Analysis Report - LEO Case,
GMV-EUM-AADD-TN2, 17/7/2013, Issue 1.1

[5] AADD Study Cases Analysis Report - GEO Case,
GMV-EUM-AADD-TN1, 17/7/2013, Issue 1.1